Proceedings of the 20th International Conference on Soil Mechanics and Geotechnical Engineering– Rahman and Jaksa (Eds)

S-wave velocity assessment using time-scale approaches with wavelets

Alfonso Fernández-Lavín & Efraín Ovando-Shelley
Instituto de Ingeniería, Universidad Nacional Autónoma de México, Circuito Escolar s/n, Ciudad Universitaria, Mexico City, 04510, Mexico

ABSTRACT: Many phenomena in nature can be represented as time series, and it is frequently necessary to know how their frequency content varies with time. If the time series is non-stationary and transient, this type of analysis can be performed using the wavelet transform. This approach allows a local analysis within windows having different frequency ranges. In this article, continuous and discrete wavelet transforms are used following different approaches to analyze output signals generated with bender elements placed on Texcoco clay samples tested in an instrumented triaxial cell, to assess the S-wave arrival time. Travel times were regarded as: a) a specific event with a high relative value of energy at a specific time in different levels; b) a maximum peak in a time-scale-coefficients diagram, and c) a relative peak in a reconstructed output signal using wavelet coefficients that were previously filtered with a threshold filter. It is shown that S-wave arrival times obtained with those approaches can be slightly dissimilar because they use different selection criteria, and besides, different types of mother wavelets were applied to obtain the wavelet coefficients. S-wave velocities (Vs) assessed with the different wavelet transform approaches are also compared with those evaluated from a resonant column apparatus, showing that, in general, Vs values agree well.

KEYWORDS: Bender elements; wavelet transform; S-wave velocity; triaxial test; resonant column.

1 INTRODUCTION

An accurate evaluation of dynamic properties of a soil stratum such as the small-strain shear modulus, damping ratio, Poisson's ratio, and natural density is an essential issue for soil characterization. There are different field and laboratory techniques to evaluate the soil behavior in the linear elastic range (small strain), being the maximum shear stiffness (G_{max}) a widely studied parameter. G_{max} evaluation can be relatively simple (Eq. 1) when S-wave velocity (Vs) and the total mass density of the soil (ρ) are previously known.

$$G_{máx} = \rho Vs^2 \tag{1}$$

The piezoelectric transducers are a laboratory technique that has been gaining popularity to study Vs because they can be installed in conventional laboratory equipment. Furthermore, Vs can be acquired in different test stages in addition to the classical mechanical parameters (Cázarez, et al., 2018). Bender elements (BE) are piezoelectric transducers installed as a cantilever beam to generate S-waves; they produce an electrical signal when are subjected to mechanical deformation and vice versa (Brignoli, et al., 1996). To assess Vs with this technique, it is necessary to know only the length (L) and the time (t) required by the S-wave to travel across the soil specimen. In the last decades, many researchers have been focused on discussing diverse interpretation methods both in the time domain (TD) and the frequency domain (FD). Different values of Vs can be achieved depending on the used interpretation approach (Viggiani & Atkinson, 1995; Kawaguchi, et al., 2001; Viana da Fonseca, et al., 2009; Yamashita, et al., 2009).

In order to explore new approaches to estimate t, the wavelet transform has been used in BE tests. It has been observed that the S-wave travel time measured is less susceptible to the influence of noise and near-field effect (Brandenberg, et al., 2008; Bonal, et al., 2012) even though these approaches involve extremely complicated algorithms.

In this paper, the theory of the wavelet transform is presented, and different methods are presented to assess the S-wave arrival time in BE tests that have been recently developed by the authors. The S-wave velocities were acquired from lacustrine soil specimens that were tested in a triaxial cell equipped with BE (vertical wave propagation). Vs assessed using the different wavelet transform approaches are also compared with those evaluated from a resonant column apparatus, showing that, in general, Vs values agree well.

2 THE WAVELET TRANSFORM

The wavelet transform is the inner product of a function $f(t)$ with a family of functions $\psi_{a,b}$ that depends on two variables. The function ψ is the mother wavelet, and it is presented in Eq 2.

$$\psi_{a,b}(t) = \frac{1}{\sqrt{\lambda}}\psi\left(\frac{t-b}{a}\right) \tag{2}$$

Parameters a and b are called the scale and translation parameters, respectively. Usually, only positive scale factors are used. When $a > 1$, the wavelets dilate (wide wavelets), and for $a < 1$, the wavelets contract (narrow wavelets) although they always maintain the same shape regardless of their specific size. Even though there is no direct relationship between the scale parameter (a) and the frequency parameter (ω) used in the Fourier transform, a heuristic relationship can be established between them (Priestley, 1996). In wavelet transform, low-frequency components are sampled at large time intervals while high-frequency components are sampled at small time intervals. More comprehensive detail of the wavelet transform theory can be found in several specialized publications (Percival & Walden, 2000; Gallegati & Semmler, 2014).

To analyze discrete signals, conveniently parameters a and b take discrete values resulting in the discrete wavelet transform (DWT). In this case, a and b both take only discrete values. If a_0 and b_0 are fixed values then $a = a_0^m, b = nb_0a_0^m, n, m = 0, \pm1, \pm2, \ldots$, the discrete expression of the wavelet transform is achieved (Eq. 3).

$$\psi_{m,n}(t) = a_0^{-m/2}\psi(a_0^{-m}\, t - nb_0) \tag{3}$$

Different values of m correspond to wavelets of different widths, and a dyadic wavelet series is obtained. The signal is divided into wavelet coefficients that retain all time-domain

information with coarse resolution as the scale level increases. The oldest example of a function for which $a_0 = 2$ and $b_0 = 1$ is the Haar function with which a function can be approximated by linear combinations (Daubechies, 1992).

For coefficients calculated using the Haar wavelet (DWT), the time and scale are independent variables. Two sets of coefficients compose a wavelet level; the first consisted of the low-frequency information called the approximation coefficient (*a*) or scale coefficient (Eq. 4). The second contained the high-frequency information called the detail coefficient (*d*) or wavelet coefficient (Eq. 5).

$$a(j+1,i) = \frac{1}{\sqrt{2}}[S(j,2i-1) + S(j,2i)] \quad (4)$$

$$d(j+1,i) = \frac{1}{\sqrt{2}}[S(j,2i-1) - S(j,2i)] \quad (5)$$

where i represents the position in time from i=0 to $(2^{J-j} - 1)$, j is the scale index or transformation level, and it varies from j=0 to (J-1). The maximum number of transformation levels can be defined by specific requirements or by the data length (N), that is, $J = Log_2(N)$

3 S-WAVE ARRIVAL TIME ASSESSMENT IN BE TESTS USING THE WAVELET TRANSFORM

3.1. As the first peak in a time-scale-frequency diagram

A mother wavelet must have an average value of zero and rapidly decay its value. A wavelet commonly used in seismic engineering is known as the Ricker pulse or Mexican hat. This wavelet has no scale function, and it is derived from a function that is proportional to the second derivative of a Gaussian function; the expression of this wavelet is presented in Eq. 6.

$$\psi(x) = \frac{2}{\sqrt{3}}\pi^{-\frac{1}{4}}(1-x^2)e^{-\frac{x^2}{2}} \quad (6)$$

This prototype wavelet has been selected because its shape closely resembles the initial shape of an output signal where the S-wave arrival takes place. On the wavelet transform, a scaled version of a prototype function is translated along the time axis and a wavelet coefficient is calculated. The coefficients show the similarity between the prototype function and the analyzed signal at a specific scale and time. Using this approach, it is possible to analyze a time series in three coordinate axes (time, scale or frequency, and coefficients) called a scalogram (Fig. 1). This scalogram allows to evaluate the first S-wave arrival time since this event produces a first peak (coefficients) and its location concerning the time axis is taken (Fernández-Lavín & Ovando-Shelley, 2019a)

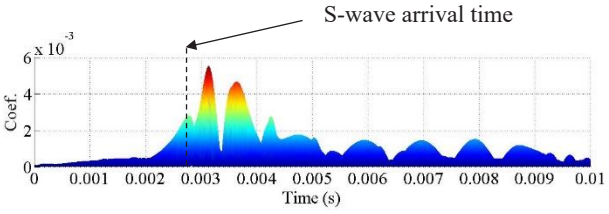

Figure 1.- S-wave arrival time evaluated using a wavelet scalogram

3.2. Using the threshold method on wavelet coefficients

Output signals can be easily contaminated by noise during signal acquisition. An output signal (*Re*) can be decomposed into the sum of the signal without noise (*S*) and noise (*Rs*) and it is presented by the Eq. 7.

$$Re = S + Rs \quad (7)$$

Frequently, the threshold method is used due to its speed and simplicity. In this approach, all wavelet coefficients at each level of the decomposition less than the threshold are set to zero and all remaining coefficients retain their value. The thresholding wavelet coefficient is appealing because it captures information at different combinations of time and frequency (scale), thus it is locally adaptive (Gencay, et al., 2002). It is reasonable to assume that only a few large wavelet coefficients contain information about the underlying function, while small coefficients can be attributed to other events. Once the small coefficients are removed, the signal can be reconstructed using the inverse discrete wavelet transform (IDWT).

This approach can be applied to BE tests within a multiresolution approach because the S-wave arrival time can be associated with a relatively high value of energy. Once the wavelet coefficients are calculated using Eq. 4 and Eq. 5, the first S-wave arrival time is reflected as large wavelet coefficients (first peak) and the smaller wavelet coefficients, that are not related with this event, are removed. Then, using the IDWT, it is possible to reconstruct the output signal to evaluate the S-wave first arrival as can be seen in Fig. 2 (Fernández-Lavín & Ovando-Shelley, 2019b).

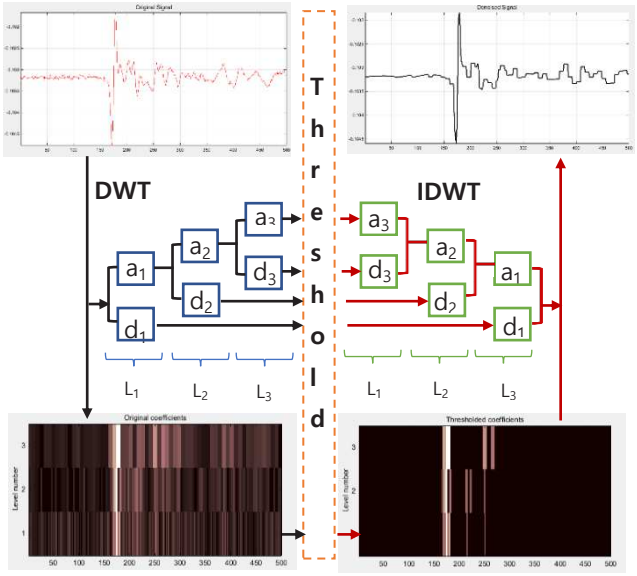

Figure 2.- S-wave arrival time using a threshold

3.3. As a maximum energy peak concerning the average energy contained in a wavelet level

In this approach, it is necessary to calculate the approximation and detail coefficients (Eq. 4 and Eq. 5) for the different levels (j = 1 - 8). The sum of the coefficients obtained from this transformation allow to express the initial function as: $f(t) = a(8) + d(8) + d(7) + d(6) + d(5) + d(4) + d(3) + d(2) + d(1)$. Based on the information of the multi-resolution analysis contained in each level, the assessment of the S-wave arrival time on the output signal cannot be made visually, and it is necessary to calculate the variance in each level analyzed using Eq 8.

$$E(j) = \sum_{i=0}^{2^{J-j}-1}[d(j,i)]^2 \quad (8)$$

where, $E(j)$ is the energy of level j, and the sum of squared

wavelet coefficients over the scales provides an orthogonal decomposition of the total sampled signal.

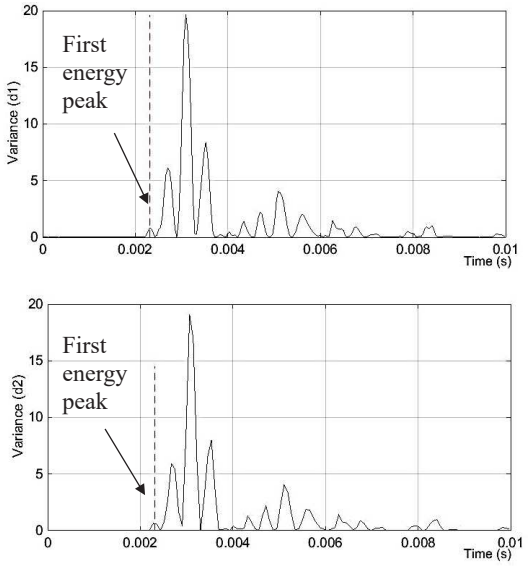

Figure 3.- Locations of energy peaks (j = 1 and j = 2).

The S-wave arrival time is associated with a relatively high value of energy because this specific event contributes more than the average energy over time in a level j; it means that there exists a singularity as a function of time (the first energy peak in the time axis). Once the variance is obtained, the different values of energy contained in the obtained levels (j=1 to 8) can be calculated using Eq 9. To establish the point of the first arrival, it is necessary to find the position of the first relative peak on the time axis, corresponding to S-wave arrival time (Fernández-Lavín & Ovando-Shelley, 2020) and it is shown in Fig. 3.

$$e(j)= \frac{[d(j,i)]^2}{\frac{1}{2^{J-j}}\sum_{i=0}^{2^{J-j}-1}[d(j,i)]^2} \quad (9)$$

4 SOIL SPECIMENS, LABORATORY EQUIPMENT, AND EXPERIMENTAL PROCEDURE

Testing was performed using soil specimens trimmed from an undisturbed lacustrine sample that was retrieved from the upper clay formation (FAS) at the former Texcoco Lake (east of Mexico City); FAS has an average thickness of 30 m and evolved from fine volcanic ash and pyroclastic materials carried by the wind; whether this period coincided with a volcanic eruption, these deposits could even be covered by volcanic sand (Zeevaert, 1983). The lacustrine deposits were deposited on the water bodies of different lakes existing at the time; this process was not continuous, and in severe low–water level periods, the sun desiccated the exposed strata, forming hardened crusts. These deposits are a widely studied geomaterial (Jaime, 1987b; Romo & Ovando-Shelley, 1996; Ovando-Shelley, 2011) and are characterized by very low shear strengths and rather a large compressibility; they have been also pointed out as extremely plastic clays. The minerals in the clay fraction can include calcium montmorillonite, sodium montmorillonite, plastic kaolin, illite, sepiolite, and attapulgite (Almanza-Hernández, et al., 2013).

The soil specimen had a natural water content of 254.8 %, a liquid limit of 247.5 %, a plasticity index of 158.7 %, a specific gravity of 2.6, a void ratio of 6.5, and their dimensions were 85 mm high and 35 mm in diameter.

The equipment used in this study includes an ELE triaxial cell equipped with BE installed in the bottom pedestal (transmitter) and top cap (receiver) connected with coaxial cables to the peripheral equipment. The setup for these tests consists of a triaxial cell provided with a submersible load cell, a Linear Variable Differential Transformer (LVDT) to measure the axial deformation, two water pressure sensors (backpressure and pore water pressure), a transducer for cell pressure, a transducer for specimen volume changes, and a pressure control panel. The triaxial control system was developed by the Engineering Institute of the National Autonomous University of Mexico (II-UNAM).

The BE dimensions were 12 x 6 x 1 mm and were covered with conductive paint to ground it and photosensitive paint to waterproof and isolate. The peripheral equipment consists of a function generator coupled to an oscilloscope model HP54540A to visualize the signals that were subsequently acquired, stored, and analyzed on a computer.

In the triaxial cell, confining pressure and backpressure were applied to the soil specimens to reach full saturation (maintaining effective stress of 10 kPa). Output signals were obtained at each confining stress level under undrained conditions once the primary consolidation was achieved (14.7, 29.4, 44.1, 68.7, and 98.1 kPa). Single-period sinusoids at various preset frequencies were selected to generate the output-analyzed signals (1, 2, 3, 4, 5, 6, and 7 kHz).

After the time series were generated, the signal processing was performed on a user-friendly interface software. The software decomposes the output signal into wavelet coefficients (CWT or DWT) and using the different approaches presented in this paper, displays results for the user to select the points used to calculate the S-wave travel time. This data is saved in a tab-delimited text format and it can be imported into a spreadsheet program to evaluate trends in the tests (Fernández-Lavín, 2020).

Furthermore, a twin soil specimen was tested in a fixed-free type resonant column; the bottom end of the soil specimen is fixed, and the top end is vibrated with different frequencies until the first mode resonance is found. This test was carried out, following the same pre-established effective stresses used previously in the triaxial cell.

5 RESULTS AND ANALYSIS

In sections 3.1, 3.2, and 3.3, different approaches were presented to evaluate the S-wave travel times in tests with BE, using the wavelet transform. To demonstrate the consistency of those methods, output signals were generated at different input frequencies and different effective stress and typical output signals are presented in Fig. 4 (14.72 kPa). Moreover, it can be seen in Fig. 4 that for an input frequency equal to 1 kHz, the output signal is influenced by the near field-effect and it has an important impact on the waveform; as the frequency of the input signal increases, this effect tends to decrease even though the signal amplitude decreases due to the signal attenuation. For each set of BE signals, the Vs were evaluated using the wavelet transform approaches, and the resulting data is analyzed and presented below.

Using the continuous wavelet transform (CWT), the S-wave arrival time is evaluated by identifying on the time axis, the first peak obtained in a time-frequency-coefficients analysis (section 3.1). As can be seen in Fig. 5, for an input frequency f = 1 kHz, Vs is determined to be 44.2 m/s although the Vs varies slightly when the input frequency is modified (f > 3 kHz) and an average S-wave velocity of 51.7 m/s was obtained that can be taken as representative of this effective stress. Furthermore, as seen in Fig. 4, the amplitude of the output signals decreases as the input frequency is increased, increasing the noise that can mask the S-wave arrival time. It is essential to highlight that this technique

allows evaluating Vs in output signals influenced by noise because a multi-resolution analysis breaks up signal components in different frequency bandwidths (different scales), retaining the high-frequency components (noise) at the lowest levels. As wavelet transformation levels increase, the information representing the S-wave arrival time can be identified, and Vs does not undergo significant changes from the average value.

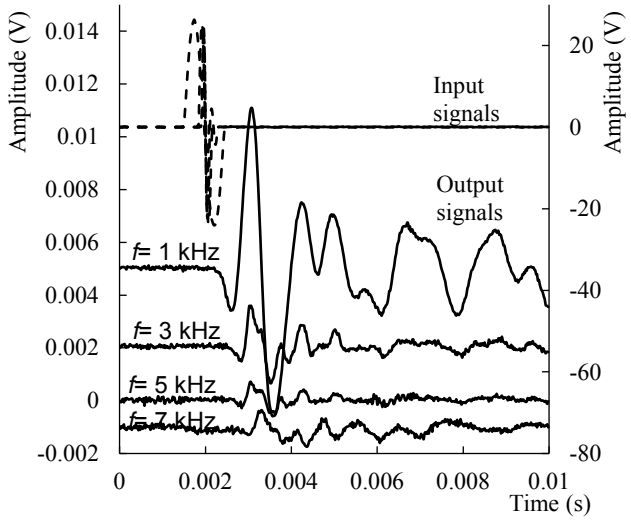

Figure 4.- Output signals generated with different effective stress (*f*=4 kHz)

In output signals reconstructed from filtered wavelet coefficients using the soft threshold criterion (section 3.2), the S-wave arrival time is evaluated. It is seen in Fig. 5 that for an input frequency f = 1 kHz, the Vs calculated is 43.2 m/s even though the S-wave velocity increases as the input frequency increments from 48.54 m/s (f = 2 kHz) to 52.58 m/s (f = 7 kHz) and an average Vs of 50.9 m/s is selected as representative for this effective stress state. This increase may have been due to noise in the output signals because the filtering threshold is proportional to the Gaussian distribution of the wavelet coefficients. As the noise is increased due to the signal attenuation, also the high-frequency component increases, modifying the threshold boundaries.

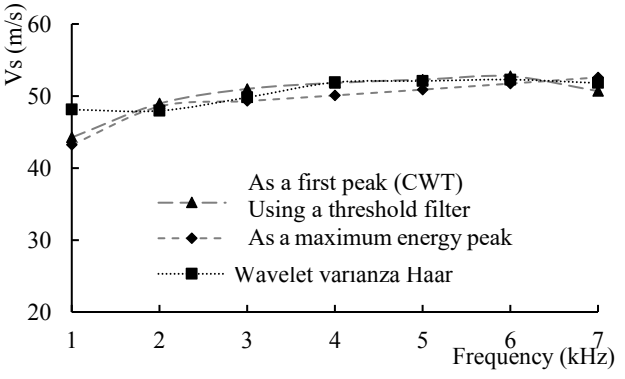

Figure 5.- Vs results for input sine waves of 1 to 7 kHz assessed with different wavelet approaches

On the other hand, to evaluate Vs, the S-wave travel time was assessed as a maximum energy peak concerning the average energy contained in a wavelet level (section 3.3). As seen in Fig. 5, the S-wave velocity varies between 47.95 m/s and 50.08 m/s regardless of the input frequency; therefore, the dependence of Vs on input frequency appears to be minimal. Averaging the values assessed using this approach, an average S-wave velocity of 50.9 m/s was calculated that is representative of this stress state. Moreover, an important characteristic of this method is that it allows evaluating output signals even influenced by the near field effect.

In general, it is observed in Fig. 5 that the scatter of Vs data is higher when the input frequency is less than 3 kHz. In lacustrine soils of the Mexico Valley, it has been observed that if the frequency of the input signal (one cycle of a sinusoidal input) is higher than 4 kHz, it is possible to avoid the near-field effects on the output signal; in other words, L/λ becomes independent of frequency (Fernández-Lavín & Ovando-Shelley, 2020).

Figure 6 shows results for the Vs obtained in the resonant column test for different effective stresses that are compared with those evaluated with the wavelet transform. Two limiting lines of Vs are also illustrated (minimum and maximum Vs values) to observe that the S-wave velocities using the wavelet transform methods in the current test series have a difference of only 5 m/s regardless of the effective stress. For confining stress less than 44.15 kPa, the Vs evaluated with any wavelet transform technique is like each other, and additionally, they are remarkably close to the Vs obtained in the resonant column test. On the other hand, for confining stresses greater than 44.15 kPa, this difference increases gradually until reaching its maximum value in the confining stress of 98.1 kPa, where the estimated Vs with BE are less than the Vs of the resonant column. The Vs obtained with the energy approach (relative value of variance) are in the upper limit concerning the other approaches, regardless of the confining stresses applied to the soil specimen, as shown in Fig. 6. Furthermore, the Vs obtained with the criteria of the wavelet coefficient and the reconstruction of the signal from filtered coefficients are in the central part of the general trend.

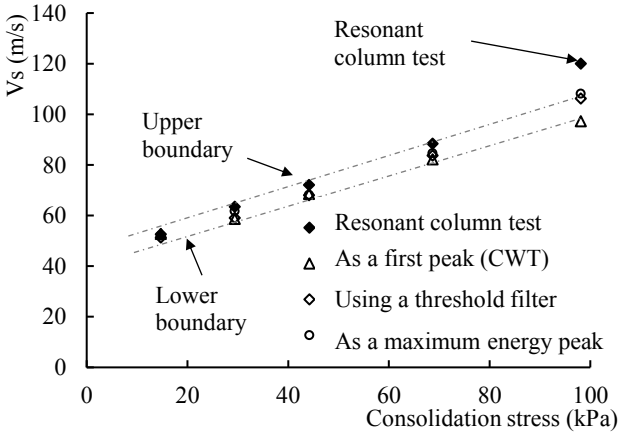

Figure 6.- S-wave velocity with wavelet approaches and the resonant column test

As reported in Fig. 6, there is a slight difference between the estimated Vs with the BE and the resonant column due to the fundamental principles involved in test methods. The BE measures the local stiffness of the soil specimen, and this technique is based on the evaluation of elastic waves locating stiffness along the wave propagation path (vertical propagation). Otherwise, the resonant column test measures the average and representative stiffness of the entire soil specimen at small deformations caused by charge-discharge cycles.

S-wave velocities presented in Fig.6 show scattered Vs from the wavelet transform approaches because each technique is based on different criteria to select the S-wave arrival time on the time axis; it is essential to consider that the wavelet coefficients are obtained with different mother wavelets. Indeed, a Haar wavelet was used for DWT analysis, and a Mexican hat pulse was employed for the CWT calculation. If these prototype

functions were modified, the Vs could also vary moderately because, depending on the specific characteristics of the analyzed output signal, a specific mother wavelet can highlight and identify different singularities of the waveforms.

6 CONCLUSIONS

This study aims to evaluate the S-wave travel time in bender elements tests using the wavelet transform. These techniques allow to analyze an output signal within a multiresolution approach, and they can be used even in signals affected by noise or the near-field effect that normally hides the S-wave arrival. The main findings of this study include:

- Regardless of the consolidation stress during the triaxial test, the output signals are significantly influenced by the input frequency. For an $f < 4$ kHz, the near-field effect is observed, but as the input frequency has been increased, this effect tends to disappear. The near-field effect influences the Vs evaluated as the first peak in a time-scale-frequency diagram and signals reconstructed from filtered wavelet coefficients. In contrast, the Vs estimated as a maximum energy peak concerning the average energy contained in a wavelet level is not dependent on the input frequency.
- S-wave velocities obtained with the wavelet transform methods in the current test series have a difference of only 5 m/s regardless of the effective stress, and they were essentially the same as those obtained in the RC test.
- Fig. 7 shows Vs obtained with different wavelet approaches to select the S-wave arrival time and types of the mother wavelet. On the one hand, the Haar wavelet was used in the analyses carried out with the DWT, and, on the other hand, a Mexican hat wavelet was used for the analysis executed with the CWT. The wavelet transform allows selecting different types of essential functions that are compared with the waveform under analysis, and a specific mother wavelet can highlight and identify different singularities of the waveforms. Indeed, if these basic functions were modified, the results presented in Fig. 7 could also vary moderately.

7 ACKNOWLEDGEMENTS

The authors gratefully acknowledge the financial support of the CONACYT and the UNAM Engineering Institute. Moreover, A. Fernández-Lavín also thanks to SENESCYT (Ecuador).

8 REFERENCES

Almanza-Hernández, F., Rangel-Nuñez, J. and Garfias-García, E., 2013. Study on the composition and microstructure of lacustrine soft soil deposits in Mexico City. *In Proceedings of the ISSMGE Technical Committee TC-214 Workshop Extreme Soils Mechanics, México City, 23 May 2013. SMIG*.

Bonal, J., Donohue, S. and McNally, C., 2012. Wavelet Analysis of Bender Element Signals. *Géotechnique,* 62(3), 243-252.

Brandenberg, S. J., Kutter, B. L. and Wilson, D., 2008. Fast Stacking and Phase Corrections of Shear Wave Signals in a Noisy. *Journal of Geotechnical and Geoenvironmental Engineering,* 134(8), 1154-1165.

Brignoli, E. G., Gotti, M. and Stokoe, K. H. I., 1996. Measurement of shear waves in laboratory specimens by means of piezoelectric transducers. *Geotechnical Testing Journal,* 19(4), 384-397.

Cázarez, I., Fernández-Lavín, A. and Ovando-Shelley, E., 2018. Determinación de velocidades de ondas: cortante (Vs) y de compresión (Vp), en muestras de suelos pre consolidados y normalmente consolidados del Ex Lago de Texcoco. In *Proc.of the XXIX Reunión Nacional de Ingeniería Geotécnica, 23 y 24 Noviembre 2018, León, Guanajuato, México[in spanish].*

Daubechies, I., 1992. *Ten lectures on wavelets.* Philadelphia, PA: Society for Industrial and Applied Mathematics.

Fernández-Lavín, A., 2020. Interpretación de señales: uso de transformada wavelet para obtener parámetros dinámicos en suelos. *PhD Thesis, Universidad Nacional Autónoma de México, México[in spanish].*

Fernández-Lavín, A. and Ovando-Shelley, E., 2019a. Interpretación de señales usando transformadas wavelet continuas. In *Proc. of the XVI Pan-American Conference on Soil Mechanics and Geotechnical Engineering, 17-20 November 2019, Cancun, Mexico [in spanish].*

Fernández-Lavín, A. and Ovando-Shelley, E., 2019b. Método de filtrado con wavelet para el análisis de señales. In *Proc. of the XVI Pan-American Conference on Soil Mechanics and Geotechnical Engineering, 17-20 November 2019, Cancun, Mexico [in spanish].*

Fernández-Lavín, A. and Ovando-Shelley, E., 2020. Haar wavelet transform for arrival time identification in bender element tests [on line]. *Geotechnical Testing Journal,* 43(4), 937-949.

Gallegati, M. and Semmler, W., 2014. Wavelet applications in economics and finance. En: *Dynamic modelling and econometrics and finance.*Springer.

Gencay, R., Selcuk, F. and Whitcher, B., 2002. *An introduction to wavelet and other filtering methods in finance and economics.*Academic Press, Inc.

Jaime, A., 1987b. Foundation Engineering in Mexico City: General Aspects and Subsoil Conditions. *In Proc. Int. Symp. on Geotechnical engineering of soft soils, Mexico City, México,* 225-243.

Kawaguchi, T., Mitachi, T. and Shibuya, S., 2001. Evaluation of Shear Wave Travel Time in Laboratory Bender Element Test. *In Proceedings of the Fifteenth International Conference on Soil Mechanics and Geotechnical Engineering, 27–31 August 2001, Istanbul, Turkey,* 155-158.

Ovando-Shelley, E., 2011. Some geotechnical properties to characterize Mexico City Clay. In *Proc. of the 14th Panamerican conference of soil mechanics and geotechnical engineering, October 2-6, 2011, Toronto, Ontario, Canada.*

Percival, D. and Walden, A., 2000. *Wavelet Methods for Time Series Analysis.* Cambridge, UK: Cambridge University Press.

Priestley, M., 1996. Wavelets and Time-Dependent Spectral Analysis. *Journal of Time Series Analysis,* 17(1), 85-103.

Romo, M. and Ovando-Shelley, E., 1996. Modelling the dynamic behaviour of Mexican Clays. *In Proceedings of the Eleventh World Conference on Earthquake Engeenering, 23-28 June 1996, Acapulco, Mexico*.

Viana da Fonseca, A., Ferreira, C. and Fahey, M., 2009. A Framework Interpreting Bender Element Tests, Combining Time-Domain and Frequency-Domain Methods. *Geotechnical Testing Journal, ASTM,* 32(2), 91-107.

Viggiani, G. and Atkinson, J. H., 1995. Interpretation of Bender Element Tests. *Géotechnique,* 45(1), 149-154.

Yamashita, S. and other, 2009. Interpretation of International Parallel Test on the Measurement of Gmax Using Bender Elements. *Soils and Foundations,* 49(4), 631-650.

Zeevaert, L., 1983. *Foundation Engineering For Difficult Subsoil Conditions.* Van Nostrand Reinhold Company.